Observation of coherent diffraction radiation from bunched electrons passing through a circular aperture in the millimeter- and submillimeter-wavelength regions

Yukio Shibata, Shigeru Hasebe, Kimihiro Ishi, Toshiharu Takahashi,* Toshiaki Ohsaka, and Mikihiko Ikezawa
Research Institute for Scientific Measurements, Tohoku University, Katahira, Sendai 980-77, Japan

Toshiharu Nakazato, Masayuki Oyamada, Shigekazu Urasawa, and Tatsuya Yamakawa
Laboratory of Nuclear Science, Tohoku University, Mikamine, Sendai 982, Japan

Yasuhiro Kondo
Faculty of Engineering, Tohoku University, Aramaki, Sendai 980-77, Japan
(Received 19 June 1995)

Using a short-bunched beam of electrons of 150 MeV, we have generated diffraction radiation from a circular aperture in an aluminum plate in the region of millimeter and submillimeter wavelengths. We have observed superposition of the diffraction radiation and transition radiation from an aluminum mirror. The angular distribution of the observed radiation shows interference of the two radiations. The intensity of the radiation has been observed to be proportional to the square of the beam current. Compared with the theoretical intensity of incoherent radiation, the observed intensity of the radiation from an aperture of 10 mm at the wavelength of 1 mm has been enhanced by a factor of 1.5×10^8, which is roughly equal to the number of electrons in a bunch. From the observed spectrum, the longitudinal distribution of electrons in a bunch has been derived with a spatial resolution of 0.1 mm, i.e., a temporal resolution of 0.3 ps.

PACS number(s): 41.60.−m, 41.75.Ht, 42.72.Ai, 29.17.+w

I. INTRODUCTION

Diffraction radiation (DR) is emitted when an electron of a constant velocity passes by a metallic structure [1,2]. DR is an important process of energy loss of the electron, in particular when it occurs in particle accelerators. Theoretically, DR has been studied for simple structure such as a circular aperture in a metallic screen, a semi-infinite screen, and concentric cylindrical pipes with a jump in radius [1,3,4].

Experimentally, DR has hitherto been investigated for cylindrical pipes in a long-wavelength region to examine the loss of energy of an electron beam in a storage ring [5,6], and the total intensity of DR, or the radiation loss, has been evaluated in units of impedance in the microwave or longer-wavelength region. However, no observation of emitted DR has been made.

According to the theory [3], the intensity $P(D,\lambda,\theta)$ of forward DR emitted from the electron with relativistic velocity passing through a circular aperture in an ideally conducting screen is expressed as follows:

$$P(D,\lambda,\theta)=I_0(\lambda,\theta)[E(D,\lambda,\theta)]^2 , \quad (1)$$

where

$$E(D,\lambda,\theta)=J_0(\pi D\sin(\theta)/\lambda)[\pi D/(\beta\gamma\lambda)]K_1(\pi D/(\beta\gamma\lambda)) \quad (2)$$

and I_0 is the intensity of transition radiation (TR) emitted from the electron passing through the ideally conducting screen in vacuum [7]; D is the diameter of the aperture, β is the ratio of speed of the electron to that of light in vacuum, γ is the Lorentz factor, and θ is the direction angle measured from the beam axis. The functions J_0 and K_1 in Eq. (2) are, respectively, the Bessel function of the zeroth order and the modified Bessel function of the first order. Backward DR is also expressed by Eqs. (1) and (2) with the replacement of θ by $\pi-\theta$. When the size of the aperture decreases, DR approaches TR. The absolute values of the function $E(D,\lambda,\theta)$ are always smaller than unity, and in the limit of small aperture $D/\lambda\rightarrow0$, the factor E tends to unity.

Recently, using a beam of a linear accelerator, coherent radiation from a short-bunched beam of electrons, such as coherent synchrotron radiation, coherent TR, and coherent Cherenkov radiation have been observed in a region where the wavelength is longer than or nearly equal to the size of a bunch [8–11]. The intensity of the coherent radiation is proportional to the square of the beam current, and it is enormously enhanced compared with incoherent radiation. The coherent radiation is useful not only as an intense light source but also as a means of diagnostics of the electron beam. From the analysis of the coherent radiation, we can derive information on the distribution of electrons in the bunch [9,11–13]. Coherent DR is more suitable for diagnostics of the beam than other coherent radiation, such as TR and synchrotron radiation, because DR is generated by a smaller perturbation to the beam than the others.

*Present address: Research Reactor Institute, Kyoto University, Kumatori, Osaka 590-04, Japan.

 ©1995 The American Physical Society

In the present experiment, we have observed coherent DR using a short-bunched beam of a linear accelerator. Coherent DR emitted from electrons of 150 MeV passing through a circular aperture in an aluminum plate has been observed in the region of millimeter and submillimeter wavelengths. The intensity and its angular dependence of coherent DR have been investigated in comparison with those of coherent TR which is well investigated in the long-wavelength region [11].

II. EXPERIMENT

The experimental setup is schematically shown in Figs. 1(a) and 1(b) . Electrons passed through the center of a circular aperture in an aluminum disk S. Radiation emitted from the aperture was reflected by a corner reflector $M1$ to a mirror $M2$ located at the position of 40 mm below the trajectory of the electrons, and was led through a quartz window W to a grating type far-infrared spectrometer, which covered the wavelength range from 0.1 to 5 mm. The acceptance angle of the measuring system was 70 mrad. The radiation was detected by a liquid-He-cooled Si bolometer.

The corner reflector $M1$ was composed of two pieces of aluminum-evaporated fused silica glass; each of the glass has the size of $32\times50\times1$ mm^3 in width, length, and thickness. The distance between the radiator and the mirror $M1$ was 100 mm. The mirrors $M1$ and $M2$ were rotatable around a vertical axis.

As the source of DR, we prepared three pieces of aluminum disk with a central hole. The size of the disk was 50 mm in outer diameter and 2 mm in thickness; the diameters of the central hole were 10, 15, and 20 mm for the three disks. As the source of TR, a 15-μm-thick aluminum foil was also prepared. The four radiators, of which three were for the source of DR and one for TR, and a sheet of BeO film were attached to the turn table T as shown in Fig. 1(b). In the experiment, one of the radiators or the BeO film was selected to be placed on the trajectory of the electron beam by rotating the turn table driven with a pulse motor. The radiator was perpendicular to the trajectory of the beam.

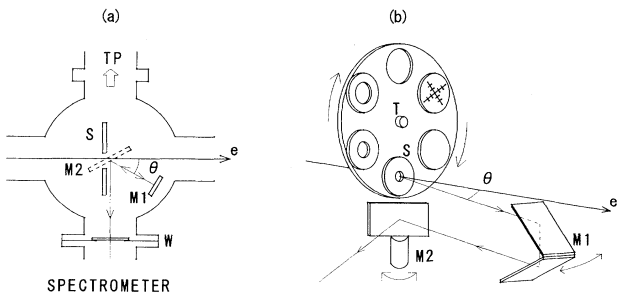

FIG. 1. Schematic diagrams of the experiment: (a) top view and (b) bird's-eye view. S, radiator; $M1$, corner reflector; $M2$, plane mirror; W, quartz window; T turn table. Electrons move along the horizontal line from left to right. Three pieces of aluminum disk with a hole, aluminum foil, and BeO film are attached on the turn table T.

The BeO film was used for the monitor of the beam position: Optical emission from the BeO film irradiated by the beam was observed with a video camera. The beam position was adjusted by a steering magnet located about 10 m upstream from the radiator.

The electrons were accelerated with the S-band linear accelerator at the Laboratory of Nuclear Science, Tohoku University. The RF frequency, the energy, and the energy spread were 2.856 GHz, 150 MeV, and 0.5%, respectively. The duration of a pulse was 5 ns and the repetition of the pulse was 25 pulses/s. The beam current was typically 10 nA; hence the average number of electrons in a bunch was 1.8×10^8. The transverse size of the beam was about 2.5 mm in diameter at the position of the radiator.

The spectral sensitivity of the measuring system was calibrated using blackbody radiation from a graphite cavity of 1200 K. Uncertainty of the absolute intensity was estimated to be a factor of 1.5.

III. RESULTS

A. Angular distribution of radiation

The angular distribution of the radiation from the circular aperture was observed by rotating the mirrors $M1$ and $M2$ in Fig. 1. The radiation was emitted in two directions, i.e., to the direction of motion of electrons (forward DR) and to the direction of specular reflection of the radiator (backward DR).

When we observed forward DR at a small angle θ in the configuration of Fig. 1, the mirror $M1$ crossed the trajectory of the beam; the mirror $M1$ thereby emits backward TR towards the observing system. Therefore the radiation observed in the range of direction angle with $|\theta|\leq9.2°$ was the superposition of forward DR from the circular aperture and backward TR from the mirror $M1$. In the measurement of the backward radiation, the mirror $M1$ also crossed the electron beam upstream from the radiator. In this case the forward TR was emitted from the mirror and was partially reflected back to the measuring system by the radiator S of DR. The radiation observed within direction angle θ of $180.0\pm9.2°$ was hence superposition of backward DR from the aperture and forward TR from the mirror $M1$.

1. Forward diffraction radiation

The angular distributions of forward DR were observed using three radiators of the apertures of 10, 15, and 20 mm, and the results are shown in Fig. 2. The observed wavelengths are 0.9, 1.3, and 2.4 mm, and the direction angle is measured from the direction of motion of the electrons. In the figure, the distribution of forward TR emitted from the aluminum foil is also shown by solid curve. Figure 2 shows that the observed radiation is symmetric with respect to the beam axis and has two peaks except for the observed distributions of the apertures of 15 and 20 mm at $\lambda=0.9$ mm. The radiation is emitted in a cone. The conical structure of the radiation at $\lambda=0.9$ mm, however, is not resolved for the two apertures, since

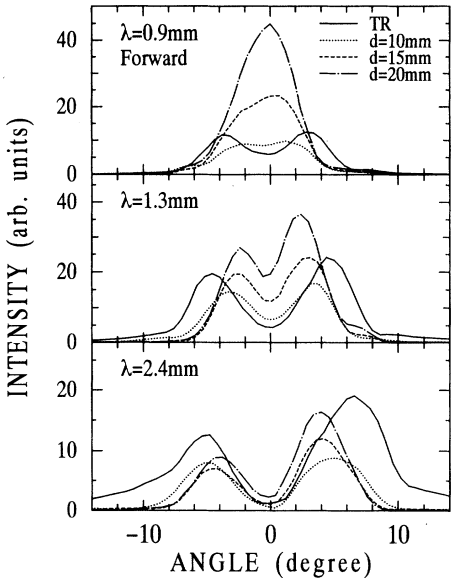

FIG. 2. Angular distributions of forward DR emitted from the circular apertures of 10, 15, and 20 mm at $\lambda=0.9$, 1.3, and 2.4 mm. The solid curve shows the distribution of the forward TR from the Al foil.

the angular resolution of the measuring system was as low as 60 mrad (3.4°).

Forward TR from the foil corresponds to the limiting case of DR in which the diameter of the aperture is negligibly small. The observed angular distributions showed the following dependence on the size of the aperture. First, the angle between the peaks decreases monotonically with the size of the aperture. Second, as the diameter of the aperture increases, the intensity of the peak decreases at first and then increases. Third, relative variation of the peak intensity is more conspicuous at shorter wavelengths. These properties are discussed in the next section.

The angular distribution of polarized components of the radiation is shown in Fig. 3 for the aperture of 15 mm. The vertical component has a central peak, whereas the horizontal component has two peaks. At the direction of the central peak $\theta=0$, the intensity of the vertical component is roughly equal to that of the horizontal one. The radiation in the direction of the peak of the total intensity is mainly polarized in the horizontal plane. This property is similar to that of TR [11].

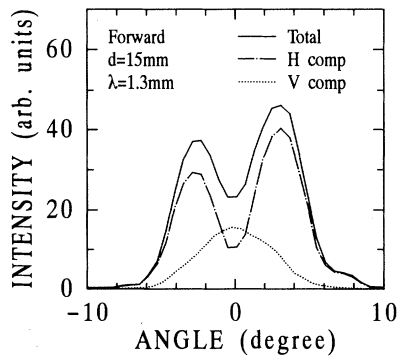

FIG. 3. Angular distribution of the polarized components of forward DR at $\lambda=1.3$ mm from the circular aperture of 15 mm. The distributions of the horizontally polarized and vertical components are shown by the dash-dotted curve and the dotted curves, respectively. The intensity of the total light is shown by the solid curve.

2. *Backward diffraction radiation*

The angular distributions of backward DR from the circular apertures of 10, 15, and 20 mm were measured at the wavelengths of 0.9, 1.3, and 2.4 mm and the results are shown in Fig. 4. In the figure, the solid curve shows the distribution of backward TR from the aluminum foil.

The distribution observed at $\lambda=2.4$ mm is symmetric with respect to the axis of specular reflection of the radiator, and has two peaks. The radiation is emitted in a cone. This property is the same as that of backward TR. The conical structure of backward DR was clearly observed also with the 10-mm aperture at $\lambda=1.3$ mm. At $\lambda=0.9$ mm, however, DR was weak, and the conical structure was not resolved.

Figure 4 shows a general tendency that both the peak intensity and the peak angle decrease with increase of the diameter of the aperture. However, it should be noted that at $\lambda=2.4$ mm the peak angle shows a slight increase with the increase of the aperture from 15 to 20 mm. The relative depression of the peak intensity is clearly seen at shorter wavelengths. The observed properties are discussed in the next section.

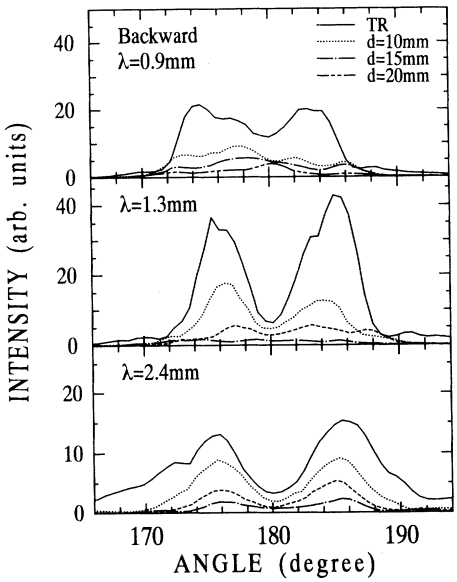

FIG. 4. Angular distributions of backward DR from the circular apertures of 10, 15, and 20 mm at $\lambda=0.9$, 1.3, and 2.4 mm. The solid curve shows the distribution of the backward TR from the Al foil.

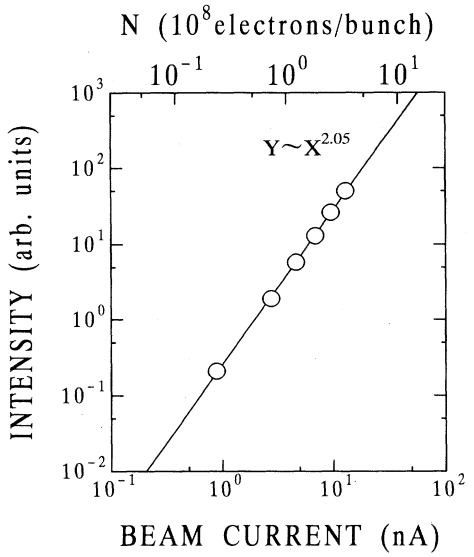

FIG. 5. Dependence of the intensity of forward DR on the beam current observed with the circular aperture of 10 mm at $\lambda=1.3$ mm. The straight line was obtained by the method of least squares.

B. Intensity-beam current relation

The dependence of the peak intensity of the forward radiation on the beam current was measured at $\lambda=1.3$ mm using the aperture of 10 mm. The beam current was varied by controlling the width of a slit located in a transport system of the beam. The position of the slit was far upstream from the measuring system shown in Fig. 1. The experimental result is shown in Fig. 5. The straight line is obtained by the method of least squares, and its gradient is 2.05. This confirms that the intensity is proportional to the square of the beam current and coherent DR has been observed.

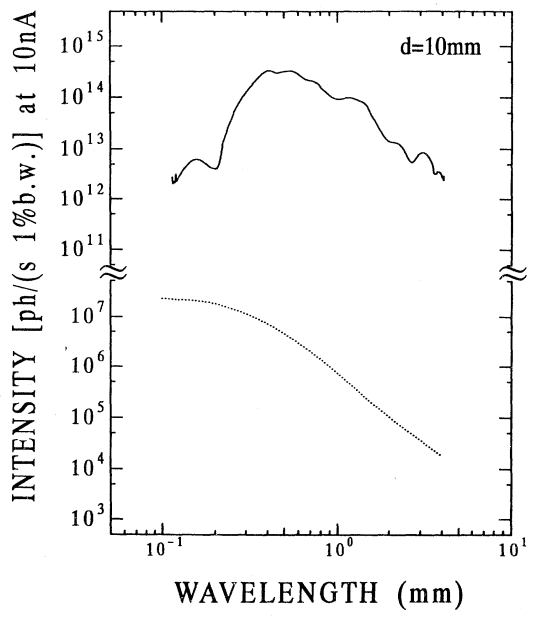

FIG. 6. Observed spectrum of forward DR from the circular aperture of 10 mm. The dotted curve is the theoretical intensity of incoherent forward radiation (see the text for detail).

C. Spectrum

Spectrum of the forward DR from the circular aperture of 10 mm was observed at the direction angle $\theta=0$, and is shown by the solid curve in Fig. 6. The ordinate shows the intensity received by the spectroscopic system with the acceptance angle of 70 mrad in units of numbers of photon per second per 1% bandwidth, i.e., $\Delta\lambda/\lambda=0.01$, on the condition of the beam current of 10 nA. The spectrum has a broad peak around at $\lambda=0.5$ mm, and the intensity decreases rapidly towards shorter wavelengths. In the long-wavelength region $\lambda>1$ mm, the intensity decreases with wavelength and it is roughly proportional to the inverse of $\lambda^{2.5}$.

IV. DISCUSSION

A. Superposition of diffraction radiation and transition radiation

1. Forward diffraction radiation

The angular distributions of DR shown in Figs. 2 and 4 are the results of the superposition of the radiations from the radiator S and the mirror $M1$ in Fig. 1. In the case of the observation of forward TR from the aluminum foil, the observed radiation is superposition of the forward TR from the foil and the backward TR from the mirror $M1$. The intensity of the superposed radiation at a far point of observation is expressed as follows [11]:

$$P=2I_0[1-\cos(L/Z)]\ , \tag{3}$$

where I_0 is TR from a single boundary, L is the distance between the aluminum foil and the mirror, and Z is the formation zone:

$$Z=\beta\lambda/[2\pi(1-\beta\cos\theta)]\ . \tag{4}$$

By analogy, superposition of forward DR and backward TR is written as follows:

$$P=I_0[1+E^2-2E\cos(L/Z)]\ , \tag{5}$$

where E is the factor $E(D,\lambda,\theta)$ expressed by Eq. (2). When the size of the aperture decreases $D/\lambda\rightarrow 0$, the factor E tends to unity and Eq. (5) reduces to Eq. (3).

The theoretical angular distribution of forward DR has been calculated using Eq. (5) and is shown in Fig. 7. In the calculation, the acceptance angle of the experimental system has been taken into account. In the figure, the theoretical distribution of forward TR is also shown by the solid curve. The calculation qualitatively reproduced the experimental results of the relative variation of the peak angle and of the peak intensity in Fig. 2. The theoretical curves in Fig. 7 showed that as the diameter increases, the peak intensity decreases first and then, after reaching a minimum value, increases. The peak angle, on the other hand, decreases monotonically with the diame-

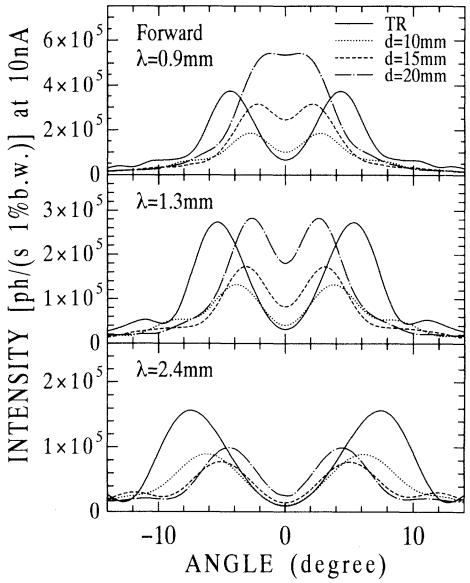

FIG. 7. Theoretical curves of angular distributions of forward DR from circular apertures of 10, 15, and 20 mm. The solid curves show the distribution of forward TR.

ter, i.e., the vertex angle of the radiation cone decreases with the size of the circular aperture. The calculated curves in Fig. 7 show good agreement with the experimental ones of Fig. 2. This result indicates that we have observed diffraction radiation emitted from the aperture which is superposed with TR form the mirror $M1$.

The experiment, however, shows small discrepancies with the theory. The variation of the peak intensity observed at $\lambda=0.9$ mm is larger than the theoretical one. The observed angular distributions from the apertures of 15 and 20 mm have only one central peak, which indicates that it is caused from rapid decrease of the vertex angle of the radiation cone. On the other hand, the theoretical curves show two peaks. The reason for the discrepancies is not clear at present.

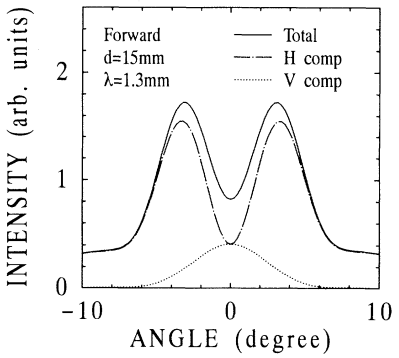

FIG. 8. Theoretical curves of angular distributions of polarized components of forward DR at $\lambda=1.3$ mm from the aperture of 15 mm. The horizontally polarized and vertical components are shown by the dash-dotted and the dotted curves, respectively. The intensity of the total light is shown by the solid curve.

Corresponding to the results of Fig. 3, we have calculated the polarized components of the intensity and the results are shown in Fig. 8. The calculation reproduced well the properties of the polarized components of the radiation described in Sec. III A 1. This confirms that the electric vector of the radiation is in the plane including the beam axis and the observation point. This property is the same as that of TR [11].

2. *Backward diffraction radiation*

In the arrangement to observe backward DR, the forward TR from the mirror $M1$ in Fig. 1 was reflected by the radiator S, i.e., the aluminum disk with the central hole. The geometrical situations are considered in the following way. We denote the limb angle of the circular aperture as θ_1, i.e., $\tan\theta_1=D/(2L)$, where D is the diameter of the aperture and L is the distance between the radiator S and the mirror $M1$. The forward TR of the mirror emitted in the direction of $\theta>\theta_1$ is reflected by the aluminum disk, and the superposition of the reflected TR and the backward DR from the aperture is observed. On the other hand, the forward TR emitted within the angle θ_1 is not reflected by the aluminum disk, and the observed radiation is only backward DR from the aperture. In this case, however, fully developed DR is not observed, because the upstream trajectory of the beam is bounded by the mirror $M1$ and the length L of the trajectory between the mirror and the circular aperture is much shorter than the formation zone of Eq. (4). At the wavelength of 1 mm, for example, the formation zone of the electron of 150 MeV is 13.7 m for the direction of $\theta=1/\gamma$. The length of the formation zone is much longer than the length L of 100 mm. When the length L of the trajectory related to emission is shorter than the formation zone, emission is partially suppressed and the radiation field is proportional to the length L [1].

The superposition of forward TR and backward DR is thus expressed as follows, on the assumption that the reflectance of aluminum is unity,

$$P=I_0[g^2+E^2G^2-2gEG\cos(L/Z)]\ , \tag{6}$$

where g is a shading factor defined geometrically and G stands for the effect of formation zone: We take $g=1$ and $G=1$ for $\theta>\theta_1$, and $g=0$, $G=\min(1,L/Z)$ for $\theta<\theta_1$, where $\min(a,b)$ indicates that we take the smaller value between a and b. In the limit of $D/\lambda\rightarrow 0$, Eq. (6) reduces to Eq. (3).

The angular distribution of the theoretical backward DR of Eq. (6) has been calculated at $\lambda=0.9$, 1.3, and 2.4 mm for the three values of the diameter of 10, 15, and 20 mm. The results are shown in Fig. 9, where backward TR is also shown by the solid curve. The intensity of radiation diminishes as the diameter of the aperture increases. The calculation has reproduced well the properties of the observed backward DR in Fig. 4. We conclude that this result verifies that we have observed backward DR from the aperture.

There remain, however, small discrepancies again between the calculation and the experiment: At $\lambda=0.9$

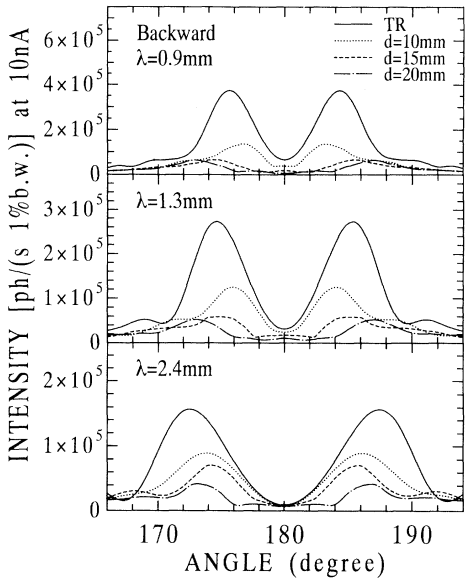

FIG. 9. Theoretical curves of angular distributions of backward DR from circular apertures of 10, 15, and 20 mm. The solid curves are the distribution of backward TR.

mm, the calculation for the aperture of 10 mm has the two peaks or the conical structure, but the experiment has not shown the peak clearly. The reason is not clear at present.

B. Spectrum and distribution of electrons in a bunch

The theoretical intensity of forward DR of Eq. (5), which includes TR from the mirror $M1$ as well, was calculated for the circular aperture of 10 mm in diameter, without the consideration of the enhancement by the coherence effect, and is shown in the dotted curve in Fig. 6. Compared with the calculation, the observed intensity is enhanced by a factor of 1.5×10^8 at $\lambda=1$ mm due to the coherence effect. The factor of the enhancement is roughly equal to the number of electrons in a bunch (1.8×10^8). In the configuration of the present experiment, the calculated spectrum decreases with the wavelength and the slope is roughly proportional to $\lambda^{-2.5}$ for $\lambda>1$ mm, as was observed.

On the analogy of coherent TR, the intensity of coherent forward DR emitted from a short-bunched beam is formulated as follows [11]:

$$P_{\text{bunch}}=PN_e^2f\ , \tag{7}$$

$$f=\left|\int S(x)\exp(i2\pi x/\lambda)dx\right|^2\ , \tag{8}$$

where P is the intensity of the superposition of DR and TR from an electron, N_e stands for the number of electrons in a bunch, and f is the bunch form factor defined by the Fourier transform of longitudinal density distribution function $S(x)$ of electrons in a bunch. In the formulation of Eq. (8) we have ignored the transverse distribution of electrons in the bunch, because the phase difference of the radiation due to the transverse spread of the electrons is small enough compared with the wavelength when we observe the spectrum in the direction of the beam axis $\theta=0$.

From the observed spectrum and the theoretical intensity of the forward DR in Fig. 6, we can derive the bunch form factor. The result is shown in Fig. 10. The value of the form factor ranges over three orders of magnitude, and in the millimeter-wavelength region it distributes irregularly around the value of unity. It is noticed that there is a small peak at $\lambda=0.15$ mm.

Distribution of electrons in a bunch has been obtained from the inverse Fourier transform of the form factor [14–16]:

$$S(x)=(2/\pi)\int[f(\sigma)]^{1/2}\cos[2\pi\sigma x-\psi(\sigma)]d\sigma\ , \tag{9}$$

where σ is the wave number of radiation; $\sigma=1/\lambda$. The phase $\psi(\sigma)$ is calculated from the observed form factor by the Kramers-Kronig relation:

$$\psi(\sigma)=-(\sigma/\pi)\int\ln[f(t)/f(\sigma)]/(t^2-\sigma^2)dt\ . \tag{10}$$

In the calculation of $S(x)$ and $\psi(\sigma)$, we need to know the value of the form factor over the entire wavelength.

Theoretically, the form factor tends to unity with the wavelength and should not exceed the value of unity. The observed form factor, however, exceeds unity in the long-wavelength region. Hence, the form factor was set equal to unity in the wavelength region longer than 1.1 mm, where the observed factor crosses over the value of unity, as shown by the dashed line in Fig. 10. The effect of this replacement is confirmed to be negligible in determining the main structure of the distribution of the electrons, as described later in this section.

The obtained distribution is shown by the solid curve in Fig. 11. The main structure of the distribution of electrons is nearly symmetric and is well approximated by a Gaussian with the bunch length [full width at half maximum (FWHM)] of 0.2 mm.

There is, however, a small bump (see the arrow in Fig. 11) on the left-hand side of the distribution function.

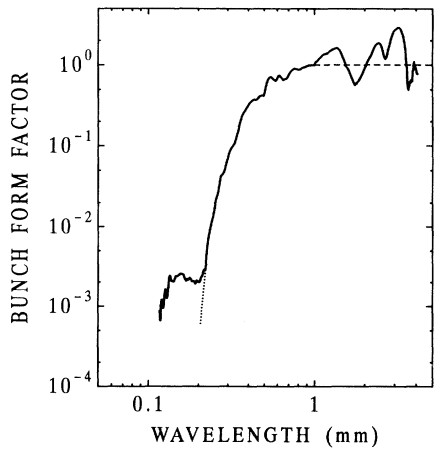

FIG. 10. The bunch form factor derived from the observed spectrum.

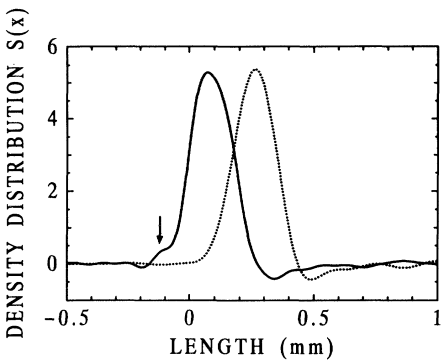

FIG. 11. Distribution of electrons in a bunch derived from the bunch form factor. The dotted curve is the distribution obtained by neglecting the small peak at $\lambda=0.15$ mm in Fig. 10, and is artificially shifted to the right by 0.2 mm.

Concerning this structure, the influence of the small peak observed at $\lambda=0.15$ mm in the spectrum was examined as follows. Ignoring the peak structure, the bunch form factor was smoothly extrapolated to shorter wavelengths as shown by the dotted curve in Fig. 10. Then the distribution of electrons was calculated using Eqs. (9) and (10). The results are shown by the dotted curve in Fig. 11, where the dotted curve is shifted to the right by 0.2 mm. The main distribution is still approximated well by the Gaussian with a bunch length (FWHM) of 0.2 mm. The small bump indicated by the arrow, however, has disappeared and the distribution has a more symmetric shape than the solid curve. The small bump has been hence confirmed to originate from the small peak of the spectrum at $\lambda=0.15$ mm.

The spatial resolution of the electron distribution in Fig. 11 is estimated from the bump structure as about 0.1 mm, i.e., the temporal resolution of 0.3 ps. The resolution is roughly equal to the shortest wavelength of the observed spectrum.

We have examined the influence of the structure of the form factor in the long-wavelength region on the distribution function, replacing the dashed line segment of $1.1<\lambda<3.8$ mm by the observed values of the form factor. No change of the nearly Gaussian distribution located around at the abscissa of 0.1 mm in Fig. 11 was recognized by the replacement. The structure of the form factor in the above-mentioned wavelength region has resulted in a change of the electron distribution in the bunch length longer than about 0.5 mm in Fig. 11.

Previously we observed spectra of coherent synchrotron radiation and of coherent TR, using the electron beam of the same linac as the present experiment. From the spectra, we obtained the results that the distribution of electrons in a bunch was approximated by a Gaussian distribution and that the bunch length (FWHM) was derived to be 0.25 mm from coherent synchrotron radiation [9] and 0.28 mm from coherent TR [11]. The main distribution of electrons derived in the present experiment from the DR is in accordance with those determined from coherent synchrotron radiation and from coherent TR. The small bump which has been clearly resolved in the solid curve of Fig. 11, however, was not obtained in the previous experiments. In the present experiment, the linac was operated in short duration of the pulse of 5 ns, whereas in the previous experiments it was operated in long duration of 2 μs. The small bump was probably caused from the change of the operational conditions of the accelerator.

DR is emitted from electrons moving in the vicinity of a metallic structure. The motion of the electrons is affected by the reaction of radiation only. Hence, emission of coherent DR makes almost no disturbance on the bunch structure and on the trajectory of the beam. Coherent DR is therefore applicable to the diagnostics of the beam during the operation of an accelerator. In the application of DR to the diagnostics of the beam, we should observe only DR to make use of the advantage of DR. Various arrangements of experiment to observe DR are conceivable; in the configuration of the present experiment, for example, by replacing the mirror $M1$ with a mirror with a central hole, we can observe superposition of DR from two apertures.

ACKNOWLEDGMENTS

We thank T. Tsutaya of the Research Institute for Scientific Measurements, Dr. Y. Suzuki and K. Shimoyama of the Faculty of Engineering, and M. Yukishima, K. Watanabe, A. Kurihara, T. Ohnuma, S. Takahashi, Y. Shibasaki, and M. Muto of the Laboratory of Nuclear Science, Tohoku University for their technical support. This work was partially supported by a Grant-in-Aid for Scientific Research from the Ministry of Education, Science, and Culture of Japan.

[1] B. M. Bolotovskii and G. M. Voskresenskii, Usp. Fiz. Nauk **88**, 209 (1966) [Sov. Phys. Usp. **9**, 73 (1966)].

[2] P. M. Van den Berg and A. J. A. Nicia, J. Phys. A **9**, 1133 (1976).

[3] Yu. N. Dnestrovskii and D. P. Kostomarov, Dokl. Akad. Nauk **124**, 792 (1959) [Sov. Phys. Dokl. **4**, 132 (1959)]; **124**, 1026 (1959) [**4**, 158 (1959)].

[4] T. Pham and R. A. Schill, Jr., J. Appl. Phys. **68**, 6010 (1990).

[5] A. Hofmann and T. Risselada, IEEE Trans. Nucl. Sci. **NS30**, 2400 (1983).

[6] A. Hofmann, IEEE Trans. Nucl. Sci. **NS32**, 2212 (1985).

[7] F. G. Bass and V. M. Yakovenko, Usp. Fiz. Nauk **86**, 189 (1965) [Sov. Phys. Usp. **8**, 420 (1965)].

[8] T. Nakazato, M. Oyamada, N. Niimura, S. Urasawa, O. Konno, A. Kagaya, R. Kato, T. Kamiyama, Y. Torizuka, T. Nanba, Y. Kondo, Y. Shibata, K. Ishi, T. Ohsaka, and M. Ikezawa, Phys. Rev. Lett. **63**, 1245 (1989).

[9] K. Ishi, Y. Shibata, T. Takahashi, H. Mishiro, T. Ohsaka, M. Ikezawa, Y. Kondo, T. Nakazato, S. Urasawa, N. Niimura, R. Kato, Y. Shibasaki, and M. Oyamada, Phys. Rev. A **43**, 5597 (1991).

[10] U. Happek, A. J. Sievers, and E. B. Blum, Phys. Rev. Lett. **67**, 2962 (1991).

[11] Y. Shibata, K. Ishi, T. Takahashi, T. Kanai, F. Arai, S. Kimura, T. Ohsaka, M. Ikezawa, Y. Kondo, R. Kato, S. Urasawa, T. Nakazato, S. Niwano, M. Yoshioka, and M. Oyamada, Phys. Rev. E **49**, 785 (1994).

[12] Y. Shibata , T. Takahashi, T. Kanai, K. Ishi, M. Ikezawa, J. Ohkuma, S. Okuda, and T. Okada, Phys. Rev. E **50**, 1479 (1994).

[13] T. Nakazato, M. Oyamada, S. Urasawa, T. Yamakawa, Y. Shibata, K. Ishi, S. Hasebe, M. Ikezawa, Y. Kondo, Y. Suzuki, K. Shimoyama, H. Hayano, T. Naito, J. Urakawa, and M. Yoshioka, in *Proceedings of the 1994 International Linac Conference, Tsukuba, Japan,* edited by K. Takata, Y. Yamazaki, and K. Nakahara (National Laboratory of High Energy Physics, Tsukuba, 1994), Vol. 2, p. 890.

[14] R. Lai and A. J. Sievers, Phys. Rev. E **50**, R3342 (1994).

[15] R. Lai, U. Happek, and A. J. Sievers, Phys. Rev. E **50**, R4294 (1994).

[16] T. Takahashi, Ph.D. thesis, Tohoku University, 1995 (unpublished).